

## Carrier recombination near threading dislocations in GaN epilayers by low voltage cathodoluminescence

N. Pauc,<sup>a)</sup> M. R. Phillips,<sup>b)</sup> V. Aimez, and D. Drouin

*Département de génie électrique et génie informatique, Université de Sherbrooke, Sherbrooke, J1K2R1 Québec, Canada*

(Received 26 April 2006; accepted 16 August 2006; published online 16 October 2006)

The authors present a low voltage cathodoluminescence (CL) study of as grown GaN and GaN:Si epilayers on sapphire. At 1 kV they resolve individual threading dislocations on the sample surface at low temperature (5 K), which appear as correlated dark spots. Analysis of CL intensity profiles across individual dislocation cores provides a direct measurement of the exciton and minority carrier diffusion lengths. Using this approach at 5 K, an exciton diffusion length of  $62 \pm 28$  nm was found for GaN:Si ( $\sim 3 \times 10^{18}$  cm<sup>-3</sup>) compared with  $81 \pm 20$  nm for a nominally undoped *n*-type GaN ( $\sim 1 \times 10^{16}$  cm<sup>-3</sup>). © 2006 American Institute of Physics. [DOI: 10.1063/1.2357881]

Due to the development of innovative growth techniques,<sup>1</sup> gallium nitride and its related compounds have become commonplace in a broad range of high power electronics and optoelectronics devices. The short carrier lifetime and the direct wide band gap of nitride materials open the door for efficient short wavelength photon devices,<sup>2,3</sup> making GaN an excellent candidate for ultraviolet solid state laser applications. However, due to the lack of a suitable growth substrate, lattice and thermal expansion coefficient mismatches between the GaN epilayer and its substrate (sapphire or SiC) persist as significant obstacles to the fabrication of high quality films. These mismatches result in a high interfacial stress in the grown layer, generating strain relieving threading dislocations (TDs) that traverse the film, emerging perpendicularly to the top surface.

It is widely accepted that TDs in GaN provide nonradiative recombination channels and charge leakage pathways.<sup>4</sup> However, no significant performance loss in GaN based optoelectronic devices is observed despite the presence of a large density of TDs. Consequently, there is a need for a detailed luminescence study of the recombination processes in the vicinity of TDs at the nanometer scale to offer a better understanding of relationships between defects and the optical properties of GaN epilayers. Earlier cathodoluminescence (CL) work, performed at 10 kV (Ref. 5) on Si doped metal-organic chemical vapor deposition (MOCVD) grown samples, reported unexpected large diffusion lengths ( $L$ ), with values lying in the same range as the dimensions of the in-plane primary electron (PE) interaction volume (IV), with a radius of  $R_e \approx 250$  nm. The experimental CL resolution is generally expressed as  $d_{CL} = 2\sqrt{R_e^2 + L^2}$ .<sup>6</sup> Considering that corresponding 300 K diffusion length measurements using electron beam induced current (EBIC) technique<sup>7</sup> give  $L \approx 100$  nm, any estimate of  $L$  at high electron beam energy becomes a difficult task because  $R_e$  and  $L$  both appreciably contribute to  $d_{CL}$ .

Low voltage (1 kV) CL can considerably improve the CL spatial resolution by reducing  $R_e$  towards a point source relative to  $L$ , producing a CL probe in a nearly pure “diffu-

sive regime.” Advances recently accomplished in the design of electron sources and electron column optics have enabled the latest field emission gun scanning electron microscopes (SEMs) to provide sub-2-nm diameter electron probes over a broad range of accelerating voltages, 1–30 kV. This capability has facilitated CL imaging and analysis of wide band gap materials with a very high spatial resolution because the IV decreases as  $\sim E^5$  with decreasing electron probe energy  $E$  and there is no corresponding increase in the electron probe diameter. In this letter we address the issues of carrier dynamics in pure and doped GaN by studying recombination processes taking place near TDs using low voltage (1 kV) temperature resolved CL microscopy and spectroscopy.

To establish a relationship between the luminescence and carrier diffusion properties of GaN as a function of their impurity content, we studied undoped and silicon doped 2  $\mu$ m thick GaN epilayers grown on (0001) sapphire by MOCVD with doping densities of  $\sim 1 \times 10^{16}$  and  $\sim 3 \times 10^{18}$  cm<sup>-3</sup>, respectively. CL studies were performed in a LEO Supra 55 VP field emission gun SEM. Samples were cleaned for 1 min in a 50 W oxygen plasma and adhered to a cold finger for low temperature measurements between 5 and 300 K. This process was found to improve the luminescence efficiency probably due to the removal of a superficial organic contamination layer.

Figures 1(a) and 1(b) show the near band edge 1 keV, 5 K monochromatic CL micrograph acquired at 361 nm— $D^0X$ —and the panchromatic (dominated by  $D^0X$  emission) micrograph on the GaN:Si and undoped GaN samples, respectively. Their general features at the micrometer scale are similar to those obtained at 10 kV (Ref. 8) with the formation of bright and smooth emitting zones separated by dark filaments but reveal a more localized and abrupt spatial modulation of the CL signal at the nanometer scale with the appearance of sub-100-nm dark spots, in contrast with completely featureless secondary electron images. These CL micrographs show a clear correlation with the EBIC images measured by Yakimov at 35 kV, where the majority of the electron beam spreading occurs in the substrate.<sup>8</sup> The dark spots observed in these images were attributed to efficient nonradiative recombination at the TDs, which locally kills the current collection in the vicinity of these defects. Similarly, in Fig. 1(a), we ascribe the isolated dark spots, resolved

<sup>a)</sup>Electronic mail: nicolas.pauc@usherbrooke.ca

<sup>b)</sup>On leave from Microstructural Analysis Unit, Faculty of Science, University of Technology, Sydney, NSW 2007, Australia.

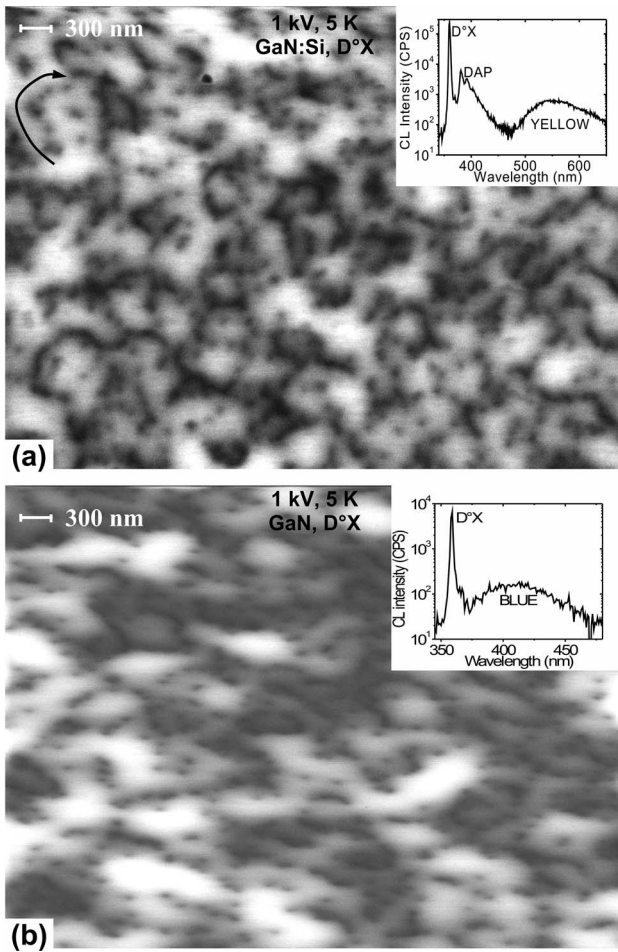


FIG. 1. CL micrographs acquired at 1 kV and 5 K on (a) GaN:Si ( $D^0X$ , 360 nm) and (b) undoped GaN ( $D^0X$ , panchromatic). Insets show the 5 K corresponding CL spectra.

chainlike dark filaments, and unresolved dark assemblies to TDs. Note that the evaluation of the TD density  $N_{TD}$  is straightforward in both samples and gives  $N_{TD} \approx 2 \times 10^9 \text{ cm}^{-2}$  and  $N_{TD} \approx 10^9 \text{ cm}^{-2}$  in the doped and undoped cases, based on a rough count of 50 and 25 pits within a 1500 nm side square, which are in good agreement with the expected  $N_{TD}$  value in GaN epilayers. The larger TD density observed in the GaN:Si specimen likely arises from Si assisted dislocation nucleation induced by extra stress in the epilayer from the dopant.

Figure 2 reports a luminescence profile measured across dislocation core—upper full curve. Also shown is a line plot—lower full curve—corresponding to the smallest measured TD core to TD core separation found in Fig. 1(b), which indicates that the spatial resolution of the CL micrograph is  $< 80 \text{ nm}$ . In the following, we will treat a TD as a one dimensional carrier sink along the  $c$ -axis growth direction with an infinite nonradiative recombination rate. This assumption is supported both by transmission electron microscopy observations of short range nanometer-extended full core screw dislocations<sup>9</sup> and by the large CL contrast observed between a dislocation core and its bright surrounding medium as shown in CL micrographs. For modeling our data, we will consider that carrier diffusion processes lead to an intensity profile of the form  $I(r) = I_0(1 - \exp[-|r - r_0|/L])$  across a dislocation core, where  $r_0$  is the core position, as observed for higher electron beam voltages.<sup>5</sup> The 1 keV ex-

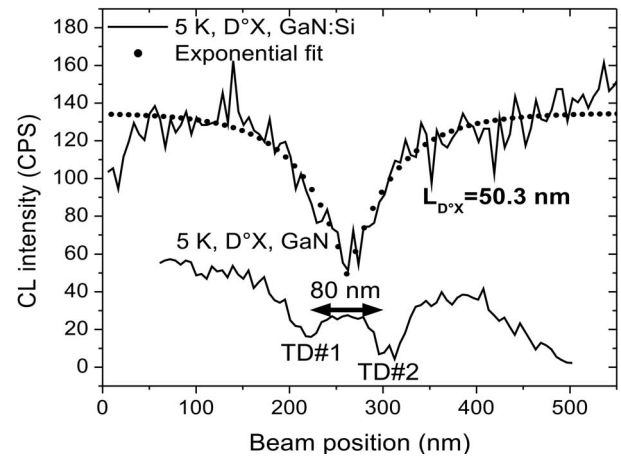


FIG. 2. Typical TD profile from Fig. 1(a) (upper full curve) with its exponential fitting curve (solid dots) and minimum TD core to core separation found in Fig. 1(b) (lower curve).

perimental CL profiles are found to follow this relationship quite well, see Fig. 2. Fitting the 5 K CL profiles with the model function for ten TDs from Figs. 1(a) and 1(b) gives the mean diffusion length of excitons using the bound exciton emission from the Si and undoped GaN, respectively, with  $L_D^{doped} \approx 62 \pm 28 \text{ nm} < L_D^{undoped} \approx 81 \pm 20 \text{ nm}$ , where the error is given by the standard deviation on the set of measures. These values are found to be much lower than previous data acquired at 10 kV (Ref. 5) and show the utility of using low voltage CL for the investigation of low  $L$  samples. The smaller mean  $L$  measured in the GaN:Si specimen is probably due to the closer mean Si to Si separation of  $\approx 10 \text{ nm}$  in the doped case, in contrast with the undoped specimen where excitons must traverse a greater distance before encountering a neutral donor. Strictly speaking, the diffusion length  $L$  entering in the CL profile represents  $d_{CL}/2$  and  $L = \sqrt{d_{CL}^2/4 - R_e^2}$ . However, since  $R_e < 8 \text{ nm}$  at 1 kV,<sup>10</sup> the reduction in the measured  $L_D^{0X}$  values is inconsequential. This latter result clearly indicates that the CL resolution at low voltage in GaN is determined by  $L$ , not  $R_e$ , because  $R_e$  can be considered to be a point source of injected carriers relative to  $L$  at 1 kV.

Figures 3(a) and 3(b) show the 360 nm— $X$ —and 382 nm—donor-acceptor pair (DAP)—CL micrographs acquired at 100 K under identical electron beam excitation conditions from the same area of the Si doped sample. While features are identical to that obtained at 5 K, one can observe a clear loss of spatial resolution in the DAP image compared with the near band edge image. Integrating the CL profile over five lines for ten isolated TDs in the doped sample gives  $L_{X-D^0X} \approx 56 \pm 14 \text{ nm}$  and  $L_{DAP} \approx 74 \pm 27 \text{ nm}$  in agreement with the image resolution observed in Figs. 3(a) and 3(b), respectively. Note that at 100 K the band edge emission arises from both free and bound excitons. Consequently, the measured diffusion length  $L_{X-D^0X}$  is thus a mixture of  $L_X$  and  $L_D^{0X}$ . The microsecond lifetime  $\tau_{DAP}$  of the DAP transition<sup>11</sup> resulting from carrier recombination on distant donor and acceptor centers is considerably larger than the lifetime of the free exciton  $\tau_X$ , which is in the 100 ps range. However, long relaxation time induced CL profile broadening in Fig. 3(b) can be ruled out because the scanning dwell time (viewed as the integration time between two consecutive

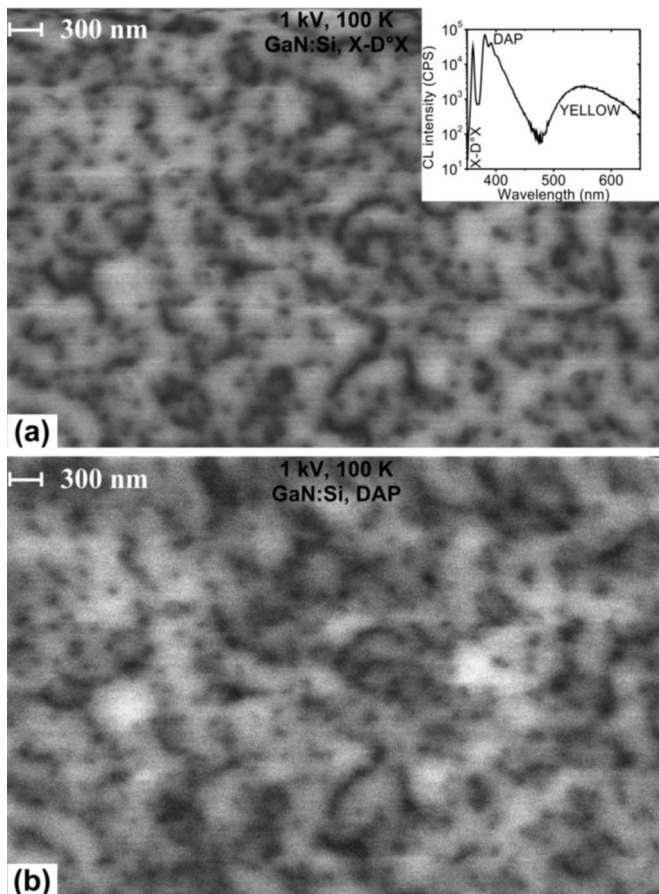


FIG. 3. CL micrographs acquired at 1 kV and 100 K on GaN:Si for (a)  $X\text{-}D^0X$  wavelength (360 nm) and (b) DAP wavelength (382 nm). Inset shows the 100 K corresponding CL spectrum.

pixels) was set to 26  $\mu\text{s}$ , which greatly exceeds  $\tau_{\text{DAP}}$ .

We can speculate that the DAP TD line profile broadening could result from donors and/or acceptors involved in the DAP recombination migrating around the TD, producing a depletion of the DAP centers within  $\sim 100$  nm radius around TD. This interpretation is consistent with recent electron energy loss spectroscopy (EELS) experiments,<sup>12</sup> which confirm oxygen segregation on TD. It should be noted that the loss in spatial resolution could also be explained by differences between the exciton and hole minority carrier diffusion lengths as well as the presence of charge at the dislocation core affecting  $L$ . However, considering the EELS results, the effect of impurity segregation seems to be the most plausible explanation for the TD broadening in the DAP images.

Observation of carrier recombination along with conservation of excitonic pairing in the first nanometers beneath the surface employing low voltage CL seems surprising at first. Surface state induced band bending, which is expected to dissociate excitons and maintain holes close to nonradiative surface traps, does not seem to play a significant role, given the relatively high intensity of measured CL signal and the very good spatial resolution observed at 1 kV. In view of the extremely high— $\sim 10^{18}$ – $10^{19}$   $\text{cm}^{-3}$ — $e\text{-}h$  pair density in the interaction volume, one can reasonably assume that efficient screening of the Coulomb interaction of trapped electrons on the surface states<sup>13</sup> by the carriers generated by the electron beam effectively flattens the upward band bending at the surface. The width of dead layer might be greatly reduced in

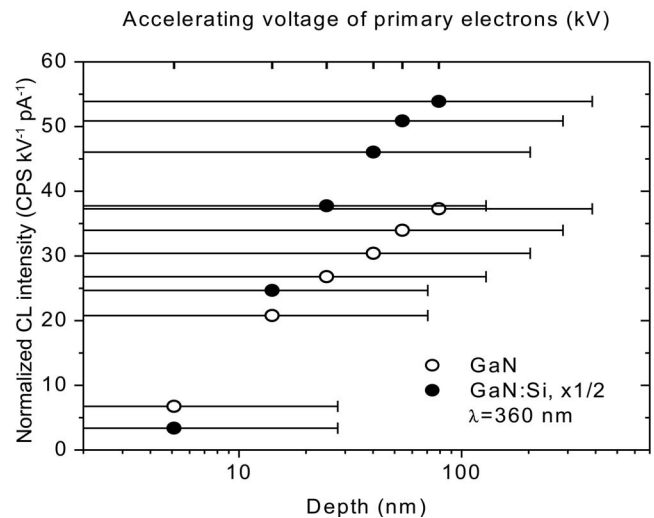


FIG. 4. Normalized CL intensity by the accelerating voltage and beam current at 360 nm as a function of the accelerating voltage (upper abscissa) and the penetration depth of PEs (lower abscissa). Bars represent the 90% cutoff of the PE energy loss distribution, and solid or open dots are centered on the maximum energy loss.

this way. Figure 4 shows the 360 nm CL intensity per unit excitation as a function of accelerating voltage. This profile reveals a significant increase of the CL intensity over the first excited 20 nm and a moderate gain as the PEs penetrate deeper in the sample, probably due to nonradiative recombination of surface carriers in the interaction volume—see horizontal bars in Fig. 4. This trend suggests that the dead layer thickness probably lies below 20 nm and does not significantly affect the CL resolution at 1 keV.

In conclusion, low voltage CL has been shown to be a powerful tool for the high spatial resolution study of TDs at GaN surfaces. CL profiles across TD cores enable direct measurement of the diffusion lengths, which have been found to be dependant on the specimen temperature and doping level. In particular, the exciton recombination length was found to be shorter in the  $n$ -type Si doped specimen when compared with a nominally undoped  $n$ -type sample, which was attributed to smaller separation between donors in the silicon doped GaN.

<sup>1</sup>A. Sakai, H. Sunakawa, and A. Usui, Appl. Phys. Lett. **71**, 2259 (1997).

<sup>2</sup>S. Nakamura, J. Cryst. Growth **201/202**, 290 (1999).

<sup>3</sup>K. Iida, T. Kawashima, A. Miyazaki, H. Kasugai, S. Mishima, A. Honshio, Y. Miyake, M. Iwaya, S. Kamiyama, H. Amano, and I. Akasaki, Jpn. J. Appl. Phys., Part 2 **43**, L499 (2004).

<sup>4</sup>L. McCarthy, I. Smorchkova, H. Xing, P. Fini, S. Keller, J. Speck, S. P. DenBaars, M. J. W. Rodwell, and U. K. Mishra, Appl. Phys. Lett. **78**, 2235 (2001).

<sup>5</sup>S. J. Rosner, E. C. Carr, M. J. Ludowise, G. Girolami, and H. I. Erikson, Appl. Phys. Lett. **70**, 420 (1996).

<sup>6</sup>S. M. Davidson, J. Microsc. **110**, 177 (1977).

<sup>7</sup>K. Kumakura, T. Makimoto, N. Kobayashi, T. Hashizume, T. Fukui, and H. Hasegawa, Appl. Phys. Lett. **86**, 052105 (2005).

<sup>8</sup>E. B. Yakimov, J. Phys.: Condens. Matter **14**, 13069 (2002).

<sup>9</sup>I. Arslan and N. D. Browning, Phys. Rev. Lett. **91**, 165501 (2003).

<sup>10</sup>We used the CASINO v244 software based on Monte Carlo simulation of PE path in the matter, [www.gel.usherb.ca/casino](http://www.gel.usherb.ca/casino)

<sup>11</sup>S. Strauf, S. M. Ulrich, P. Michler, J. Gutowski, T. Böttcher, S. Figge, S. Einfeldt, and D. Hommel, Phys. Status Solidi B **228**, 379 (2001).

<sup>12</sup>M. E. Hawkrigge and D. Cherns, Appl. Phys. Lett. **87**, 221903 (2005).

<sup>13</sup>M. A. Garcia, S. D. Wolter, T. Kim, S. Choi, J. Baier, A. Brown, M. Losurdo, and G. Bruno, Appl. Phys. Lett. **88**, 013506 (2006).